

Quantification of southwest China rainfall during the 8.2 ka BP event with response to North Atlantic cooling

Yuhui Liu^{1,2}, Chaoyong Hu¹

¹ State key lab of biogeology and environmental geology, China University of Geosciences, Wuhan, 430074, PR China

² Faculty of Materials Science & Chemistry, China University of Geosciences, Wuhan, 430074, PR China

Correspondence to: Y. Liu (yhliu@cug.edu.cn)

Abstract. The 8.2 ka BP event could provide important information for predicting abrupt climate change in the future. Although published records show that the East Asian monsoon area responded to the 8.2 ka BP event, there is no high resolution quantitative reconstructed climate record in this area. In this study, a reconstructed 10-yr moving average annual rainfall record in southwest China during the 8.2 ka BP event is presented by comparing two high-resolution stalagmite $\delta^{18}\text{O}$ records from Dongge cave and Heshang cave. This decade-scale rainfall reconstruction is based on a central-scale model and is confirmed by inter-annual monitoring records, which show a significant positive correlation between the regional mean annual rainfall and the drip water annual average $\delta^{18}\text{O}$ difference from two caves along the same monsoon moisture transport pathway from May 2011 to April 2014. Similar trends between the reconstructed rainfall and the stalagmite Mg/Ca record, another proxy of rainfall, during the 8.2 ka BP period further increase the confidence of the quantization of the rainfall record. The reconstructed record shows that the mean annual rainfall in southwest China during the central 8.2 ka BP event is less than that of present (1950 ~ 1990) by ~200 mm, and decreased by ~350 mm in ~70 years experiencing an extreme drying period lasting for ~50 years. Comparison of the reconstructed rainfall record in southwest China with Greenland ice core $\delta^{18}\text{O}$ and $\delta^{15}\text{N}$ records, suggests that the reduced rainfall in southwest China during the 8.2 ka BP period was coupled with Greenland cooling with a possible response rate of $110 \pm 30 \text{ mm}/^\circ\text{C}$.

1 Introduction

As evidence in support of global warming becomes stronger, it is apparent that the anticipated rise in sea levels may be higher than expected (Rahmstorf, 2007) and the frequency and amplitude of abrupt climate change (Martrat et al., 2004; Pall et al., 2007) may also be greater. As climate events are likely to be problematic for both ecosystems (Walther et al., 2002) and human society (Khasnis and Nettleman, 2005), any aid in prediction is crucial.

Studies of past climate events could hopefully provide useful information for exploring trigger mechanisms (Cheng, et al., 2009; Liu et al, 2013). The 8.2 ka BP event is noted to be the most pronounced abrupt climate event occurring during the whole Holocene (Alley and Ágústsson, 2005). The highest magnitude variation across the low to high latitudes makes a viable target for numerical modelings (Daley et al, 2011; Morrill et al., 2011) and may offer an insight into the sensitivity of

38 climate response in different areas (Condrón and Winsor, 2011; LeGrand and Schmidt,
39 2008). This event was firstly identified in Greenland ice cores (Alley et al., 1997),
40 showing a duration of 160-yr (Thomas et al, 2007) with a temperature drop of 3.3 ± 1.1 °C
41 in central Greenland (Kobashi et al, 2007), and is known globally (Dixit et al., 2014;
42 Morrill et al., 2013; Ljung et al., 2008; Ellwood and Gose, 2006). However, as most
43 records associated with this event mainly derived from North Atlantic and Europe
44 (Daley et al., 2011; Szeroczyńska and Zawisza, 2011; Snowball et al., 2010; Hede et
45 al., 2010; Domínguez-Villar et al., 2009; Prasad et al., 2009), the question remains as
46 to how much it influenced the East Asian monsoon area (EAMA).

47 Although some proxies from lake sediments (Yu et al., 2006; Hong et al., 2009;
48 Zheng et al., 2009; Mischke and Zhang, 2010), stalagmites (Wu et al, 2012; Cheng et
49 al., 2009; Hu et al., 2008a; Wang et al., 2005; Dykoski et al., 2005) and marine
50 sediments (Zheng et al., 2010; Ge et al., 2010) do record the 8.2 ka BP event in
51 EAMA, only Hu et al. (2008a) attempted a quantitative reconstruction of rainfall by
52 using stalagmite $\Delta\delta^{18}\text{O}$ records which indicated a decrease in precipitation during the
53 event in southwest China, an area influenced by East Asian monsoon. However, the
54 resolution of this precipitation record is approximately 100-yr and needs to be
55 improved.

56 Based on the method presented by Hu et al. (2008a), this study reconstructs a 10-yr
57 averaged annual rainfall record in southwest China during the 8.2 ka BP event by
58 comparing sub-annual (Liu et al., 2013) and 3.5-yr resolution stalagmite $\delta^{18}\text{O}$ (Cheng
59 et al., 2009) records from the same moisture transport pathway. This study further
60 addresses the sensitivity of the climate of southwest China to North Atlantic cooling
61 during the 8.2 ka BP event, providing quantitative data for simulating this global
62 event in climate system models.

63 **2 Methods**

64 **2.1 Rainfall reconstruction**

65 It has been previously discussed (Hu, et al., 2008a) that, in a monsoon area, regional
66 rainfall histories could be reconstructed by using coeval stalagmite $\delta^{18}\text{O}$ comparisons
67 between two close sites located along the same atmospheric moisture transport
68 pathway, as the difference allows the removal of secondary controls, such as moisture
69 transport and temperature on $\delta^{18}\text{O}$. Working with this premise, two published high
70 resolution stalagmite $\delta^{18}\text{O}$ sequences during the 8.2 ka BP event from Heshang cave,
71 central China (Liu et al., 2013) and Dongge cave, southwest China (Cheng et al.,
72 2009), located directly upstream in the atmospheric pathway(Fig.1), were investigated.

73 **2.1.1 Stalagmite $\Delta\delta^{18}\text{O}$ sequence establishment**

74 There is only one high-resolution $\delta^{18}\text{O}$ record from stalagmite HS4 in Heshang cave
75 ($30^{\circ}27'\text{N}$, $110^{\circ}25'\text{E}$)(Fig. 1), central China, covering the 8.2 ka BP period (Liu et al.,
76 2013), with an average resolution of ~ 0.3 -yr. However, there are two published

77 stalagmite $\delta^{18}\text{O}$ records (stalagmite DA and D4) from Dongge cave (25°17'N,
78 108°5'E)(Fig.1), southwest China (Wang et al., 2005; Dykoski et al., 2005). Cheng et
79 al.(2009) re-dated both DA and D4 from Dongge cave across the 8.2 ka BP period to
80 produce a better controlled chronology, giving $\delta^{18}\text{O}$ records with an average
81 resolution of ~3.5-yr and ~2-yr (Cheng et al., 2009) respectively. These records are
82 then compared with HS4 using the approach outlined in Hu et al. (2008a).

83 Fig. 2 shows the $\delta^{18}\text{O}$ records from HS4 (Fig. 2a) (Liu et al., 2013), DA (Fig. 2b)
84 and D4 (Fig. 2c) (Cheng et al., 2009) where similar structural patterns are observed
85 with matching major peaks and troughs. Corresponding peaks or troughs are marked
86 as shown by dashed lines in Fig. 2 and the chronology of DA, D4 and HS4 are so
87 matched to reduce the chronological uncertainty. It should be noted that the wiggle
88 matching is within the analytical uncertainty of the U-Th chronology. As the
89 measurement resolutions of HS4, DA and D4 are different, all sequences were first
90 processed to create records of equivalent annual resolution allowing the resultant time
91 sequences to be used to construct a 10-yr moving average sequence. Two $\delta^{18}\text{O}$
92 difference ($\Delta\delta^{18}\text{O}$) sequences between HS4 and adjusted DA records (Fig. 2d) and
93 between HS4 and adjusted D4 records (Fig. 2e) were thus established.

94 Though there is a systematic offset between Fig. 2d and Fig. 2e, the variations and
95 trends of the two sequences are similar, suggesting either of the two $\Delta\delta^{18}\text{O}$ sequences
96 could be used for the following reconstruction. Since the $\delta^{18}\text{O}$ record from Dongge
97 cave adopted in Hu et al.(2008a) is from DA, this study also uses data from DA (Fig.
98 2d) for further rainfall reconstruction.

99 2.1.2 Uncertainties of $\Delta\delta^{18}\text{O}$

100 The use of $\Delta\delta^{18}\text{O}$ to reconstruct regional rainfall requires some understanding of the
101 uncertainties within the measurement records and calculations. The U/Th dating
102 maximum uncertainty of stalagmite DA during the 8.2 ka BP period is ~90-yr (Cheng
103 et al., 2009), while the average difference between the adjusted and original DA data
104 set to match HS4 is ~40-yr. This adjustment is within the dating uncertainty, but to
105 test the robustness of the approach, the whole DA $\delta^{18}\text{O}$ data set is shifted by 50-yr in
106 both older and younger directions and the resultant data sets are compared. These
107 $\Delta\delta^{18}\text{O}$ sequences are shown in Fig. 3a along with unchanged DA chronology (black),
108 shifting DA 50-yr younger (blue) and 50-yr older (red). Fig. 3a suggests that though
109 the time shifted data sets show increased variability of the $\Delta\delta^{18}\text{O}$ with a maximum
110 error of 0.76‰, the general variation trends are similar, indicating that this difference
111 method is sufficiently robust for this study.

112 In addition to the chronology uncertainty, other factors may affect the accuracy of
113 $\Delta\delta^{18}\text{O}$. $\delta^{18}\text{O}$ analytical uncertainties of the HS4 and DA datasets are 0.08‰ (Liu et al.
114 2013) and 0.15‰ (Cheng, et al., 2009) respectively. Additionally the standard
115 deviation of the 10-yr average, especially the largest standard deviation of $\Delta\delta^{18}\text{O}$
116 between DA and HS4 is 0.62‰. And an estimated uncertainty of 0.35‰ from the
117 model established by Hu et al. (2008a) should be noted. Taking all of these factors

118 into consideration, the final uncertainty of the $\Delta \delta^{18}\text{O}$ sequence during the 8.2 ka BP
119 period is estimated to be $\sim 0.53\%$.

120 2.1.3 Rainfall reconstruction

121 Based on the $\Delta \delta^{18}\text{O}$ sequence shown in Fig. 3b, the rainfall during the 8.2 ka BP
122 period is reconstructed using the previous model presented by Hu et al. (2008a) via
123 the relation between $\Delta \delta^{18}\text{O}$ and rainfall ($\text{Rainfall} = 189.08 \times \Delta \delta^{18}\text{O} + 1217.4$) (Hu et al.,
124 2008a). The uncertainties from $\Delta \delta^{18}\text{O}$ give an error of ~ 100 mm/yr for the
125 reconstructed rainfall record.

126 Reconstruction of regional rainfall using two spatially separated cave records on
127 the same moisture transport pathway requires stalagmite $\delta^{18}\text{O}$ values from monsoon
128 areas to faithfully preserve rainfall information. Stalagmite $\delta^{18}\text{O}$ values are influenced
129 by different types of precipitation, along with the source and pathways of moisture,
130 plus local condensation and evaporation processes (Dayem et al., 2010). A recent
131 millennial scale climate simulation (Liu et al., 2014) suggests that Chinese stalagmite
132 $\delta^{18}\text{O}$ records might be useful as indicators of intensity of the East Asian summer
133 monsoon in terms of the continental scale Asian monsoon rainfall response in the
134 upstream regions. As both Dongge and Heshang $\delta^{18}\text{O}$ records respond to upstream
135 rainfall, the difference of the two records is expected to directly reflect the rainfall
136 between Dongge and Heshang.

137 On decadal scale, relationships between $\Delta \delta^{18}\text{O}$ and rainfall have previously been
138 discussed (Hu et al., 2008a), and we here attempt to utilize this approach on an inter-
139 annual time scale. A direct test of the validity of using moisture transport pathways
140 would use cave drip water $\delta^{18}\text{O}$ ($\delta^{18}\text{O}_d$) signals from both DA and HS4 sites which
141 should reflect speleothem $\delta^{18}\text{O}$ variations directly. Unfortunately there is no published
142 monitored data from Dongge. However there is some recently published $\delta^{18}\text{O}_d$ data
143 from a cave named Liangfeng ($26^\circ 16' \text{N}$, $108^\circ 03' \text{E}$) (Fig. 1) from May 2011 to April
144 2014 with local precipitation $\delta^{18}\text{O}$ ($\delta^{18}\text{O}_p$) data (Duan et al., 2016). Liangfeng is close
145 to Dongge ($25^\circ 17' \text{N}$, $108^\circ 5' \text{E}$) (Fig. 1) and may therefore be an alternative data source
146 to assess the validity of the rainfall reconstruction method.

147 There are three separate sequences of $\delta^{18}\text{O}_d$ from different drip sites in Liangfeng
148 cave (Zeng et al., 2015). From them, LF6 with the lowest drip rate but highest
149 variation has been selected, as it is considered to record climate information more
150 efficiently. The lowest drip rate of LF6 from Liangfeng cave suggests fresh water is
151 being mixed with delayed transit stored water for this drip site (Zeng et al., 2015) and
152 may provide longer term instead of short seasonal information compared with the
153 other two sites. Based on the 3 years of monthly monitored data of LF6 and HS4
154 (Duan et al., 2016), the sequences of annual moving average $\delta^{18}\text{O}_d$ of LF6 and HS4
155 have been calculated. Generally LF6 $\delta^{18}\text{O}_d$ values are higher than those of HS4, which
156 is sensible since Heshang cave is further along the moisture transport pathway (Fig. 1).
157 LF6 $\delta^{18}\text{O}_d$ is considered mixed fresh and stored water, so its response to the local
158 rainfall is expected to be delayed. A calculated positive correlation ($R^2 = 0.62$) between
159 the local annual moving average $\delta^{18}\text{O}_p$ and the 2-month delayed annual moving
160 average of LF6 $\delta^{18}\text{O}_d$ (monthly $\delta^{18}\text{O}_p$ and $\delta^{18}\text{O}_d$ data are from Duan et al., 2016)

161 strongly suggests that a delay of 2 months should be applied when using LF6 $\delta^{18}\text{O}_d$
162 data. A similar analysis of $\delta^{18}\text{O}_d$ at HS4 site and $\delta^{18}\text{O}_p$ outside Heshang cave (Duan et
163 al., 2016) reveals a positive correlation ($R^2=0.71$) between the local annual moving
164 average $\delta^{18}\text{O}_p$ and a 4-month delayed annual moving average for HS4 $\delta^{18}\text{O}_d$.
165 Combined analysis shows a positive correlation ($R^2=0.72$) between the 2-month
166 delayed annual moving average of LF6 $\delta^{18}\text{O}_d$ and the 4-month delayed annual moving
167 average of HS4 $\delta^{18}\text{O}_d$, giving some support to the idea that the controlling factors on
168 both LF6 and HS4 $\delta^{18}\text{O}_d$ are similar.

169 After the time adjusted $\Delta\delta^{18}\text{O}_d$ sequence has been built, the correlation between
170 $\Delta\delta^{18}\text{O}_d$ and the regional average annual rainfall at six sites between Dongge cave and
171 Heshang cave detailed in Hu et al. (2008a)(Fig. 1) may be compared. The regional
172 average annual rainfall is calculated from monthly instrumental records between May
173 2011 and April 2014 from <http://www.wunderground.com/history/>. Fig. 4 shows that
174 there is a significant positive correlation ($R^2=0.79$) between annual average $\Delta\delta^{18}\text{O}_d$
175 and regional annual rainfall, supporting the idea that the stalagmite $\Delta\delta^{18}\text{O}$ between
176 two caves located along the same moisture transport pathway can provide information
177 on regional rainfall variation.

178 2.2 Mg/Ca data processing

179 In addition to $\Delta\delta^{18}\text{O}$, the Mg/Ca ratio, another important rainfall proxy, can be
180 considered. The Mg/Ca data set is taken from Liu et al. (2013) measured using a
181 JEOL JXA8800R Electron Microprobe at the Department of Material Sciences,
182 Oxford, along the HS4 stalagmite growth axis. The Mg/Ca data were processed to
183 provide annual resolution and a 10-yr moving average constructed in the same way as
184 for $\delta^{18}\text{O}$.

185 3 Results

186 The 10-yr moving average $\Delta\delta^{18}\text{O}$ record from DA and HS4 is shown in Fig. 3b. It is
187 reasonable that the DA $\delta^{18}\text{O}$ values are generally higher than those of HS4 (Fig. 2a
188 and Fig. 2b) since Heshang Cave is located further along the moisture transport
189 pathway(Fig. 1) and is so expected to displayed a systematic $\delta^{18}\text{O}$ offset. The average
190 $\delta^{18}\text{O}$ difference between HS4 and DA is 1.0‰ during the whole Holocene (Hu, et al,
191 2008), while the average $\Delta\delta^{18}\text{O}$ value during the 8.2 ka BP event shown in Fig. 3b is
192 much lower at 0.26‰.

193 During the central event, it is notable that some of the $\Delta\delta^{18}\text{O}$ values are around
194 zero or even negative, indicating much reduced moisture transport during that time.
195 While the lowest value of $\Delta\delta^{18}\text{O}$ is nearly -0.50‰ (Fig. 3b), we do not expected
196 negative $\Delta\delta^{18}\text{O}$ values. The estimated uncertainty of ~0.53‰ in the $\Delta\delta^{18}\text{O}$ detailed
197 in section 2.1.2, along with difference in evaporation in the two caves is likely to
198 contribute to producing a negative $\Delta\delta^{18}\text{O}$. Cave monitored data suggest evaporation
199 may occur during dripping and enhanced processes in a dry season could result in
200 heavier drip water $\delta^{18}\text{O}$ values (Zeng et al., 2015), especially in a well ventilated cave.

201 Dongge is a cave consisting of branches with twists and turns, while Heshang is a
202 much simpler cave with a nearly straight main passage, and a 20 m high entrance (Hu
203 et al., 2008b). Heshang cave is clearly more open and better ventilated than Dongge
204 cave leading to greater heat and moisture exchange between the inside and outside
205 cave (Hu et al, 2008b). During similar dry conditions, the evaporation effects in
206 Heshang cave are expected to be more significant than in Dongge Cave, and the drier
207 the condition, the heavier HS4 $\delta^{18}\text{O}$ values expected, leading to lower or even
208 negative $\Delta\delta^{18}\text{O}$ values between DA and HS4. Thus less rainfall is still related to lower
209 $\Delta\delta^{18}\text{O}$ values. Since the 8.2 ka BP event is the driest period during the whole
210 Holocene (Hu et al., 2008), negative $\Delta\delta^{18}\text{O}$ values produced during the central event
211 are possible.

212 From the 10-year moving average $\Delta\delta^{18}\text{O}$ obtained from HS4 and DA records(Fig.
213 3b), there is a significant change in value from 1.3‰ to -0.5‰ over approximately 70
214 years at the commencement of the event. Compared with the average amplitude of
215 $\Delta\delta^{18}\text{O}$ during the whole Holocene of 1.0‰ (Hu et al., 2008a), this is a surprisingly
216 large change.

217 From the $\Delta\delta^{18}\text{O}$ record shown in Fig. 3b, using the previously determined relation
218 ($\text{Rainfall}=189.08\times\Delta\delta^{18}\text{O} +1217.4$) from Hu et al. (2008a), the rainfall record in
219 southwest China during the 8.2 ka BP period may be established as shown in Fig.3b.
220 While some support for the reconstruction method can be obtained using recent
221 monitoring records detailed in section 2.1.3, stalagmite Mg/Ca ratios also provide
222 some useful corroborative information.

223 Stalagmite Mg/Ca ratio is a proxy mainly controlled by local rainfall with higher
224 Mg/Ca values corresponding to lower rainfall (Fairchild and Treble, 2009), though it
225 may show some temperature dependence, increasing slightly with temperature. The
226 variation is understood to result from CO_2 -degassing occurring earlier during water
227 movement in dry seasons as cave water seeps more slowly, thus Ca is lost from karst
228 waters by formation of calcite earlier during transport processes and before waters
229 reach the stalagmite. Such a prior-calcite-precipitation process would be expected to
230 produce higher Mg/Ca ratios (Tremaine and Froelich, 2013; Fairchild and Treble,
231 2009). Although it is hard to obtain quantitative rainfall data from Mg/Ca ratios, the
232 variation of Mg/Ca may give a qualitative indication of rainfall variability and trend.
233 Therefore the variation of Mg/Ca ratios could indicate whether the reconstructed
234 rainfall from $\Delta\delta^{18}\text{O}$ is reliable or not.

235 The HS4 Mg/Ca sequence presented as a 10-yr moving average record during the
236 8.2 ka BP event is shown in Fig. 3c. As high Mg/Ca values are considered to indicate
237 low rainfall, the Y axis of Mg/Ca was reversed to make the comparison clearer. Both
238 the Mg/Ca ratios and the reconstructed rainfall data are presented as 10-yr moving
239 average values. Although the two data sets show slight differences, there is a general
240 inverse relationship between the two sequences giving a correlation coefficient (R^2) of
241 0.56 ($n=219$). And overall similarity could be observed between the trends of the two
242 patterns with high (low) Mg/Ca values corresponding to low (high) rainfall, which

243 suggests that the Mg/Ca results generally support the reconstructed rainfall record.
244 The reconstructed rainfall record (Fig. 3b) shows a maximum decline in annual
245 rainfall of 350 mm/yr, which is nearly twice that obtained from the low-resolution
246 (~100-yr) rainfall record (Hu et al., 2008a) during the same period and the lowest
247 annual rainfall in this study is lower than that from Hu et al. (2008a) by ~100 mm.
248 This is believed to be a result of the record resolution. Fig. 3b also shows that the
249 period of decreasing rainfall at the beginning of the event lasts for ~70 years, before
250 entering into an extreme dry period. During the central period of the 8.2 ka BP event,
251 the average annual rainfall is only ~1200 mm, which appears to be the driest period
252 during the whole Holocene in this area, lasting for ~50 years. The rainfall calculation
253 developed in Hu et al. (2008a) was made by averaging annual rainfall records from 6
254 sites between Heshang and Dongge(Fig. 1) and the averaged annual rainfall between
255 1950 and 1990 from the 6 sites is ~1380 mm, indicating the average annual rainfall
256 during the central 8.2 ka BP period is less than present by ~200 mm.

257 **4 Discussions**

258 It has been reported that the response of the EAMA to North Atlantic cooling during
259 the 8.2 ka BP event results from atmospheric rather than oceanic processes (Liu et al.,
260 2013). It might be assumed that the high northern latitude ice-cover reinforces
261 Northern Hemisphere cooling, increasing the temperature gradient between the high
262 and low latitudes which leads to southward migration of the inter-tropical
263 convergence zone (Chiang and Bitz, 2005; Broccoli et al., 2006). This would result in
264 weakening of the East Asian Monsoon and increased aridity. Assessment of the
265 sensitivity of southwest China climate response to North Atlantic cooling might
266 provide a clue to how North Atlantic cooling affects the EAMA.

267 Fig. 5 demonstrates three sequences of Greenland ice core $\delta^{18}\text{O}$ (Thomas et al.,
268 2007)(Fig. 5a) , a palaeo-temperature indicator (Stuiver, et al., 1995), Greenland ice
269 core $\delta^{15}\text{N}$ (Kobashi et al., 2007)(Fig. 5b), a newly developed palaeo-temperature
270 proxy (Buizert et al., 2014) and the reconstructed rainfall record in southwest China
271 during the 8.2 ka BP period(Fig. 5c). The data shown in Fig. 5a are from Thomas et al.
272 (2007) with a 3-yr resolution. To allow comparison with the reconstructed rainfall
273 records, the $\delta^{18}\text{O}$ of the ice core was processed to provide a 10-yr moving average.
274 The $\delta^{15}\text{N}$ data in Fig. 5b are from Kobashi et al. (2007) with a 11-yr resolution and
275 were processed similarly.

276 As low Greenland ice $\delta^{18}\text{O}$ and $\delta^{15}\text{N}$ values indicate local cooling (Thomas et al.,
277 2007; Kobashi et al., 2007), both Fig. 5a and Fig. 5b reveal similar trends of
278 decreasing temperature during the 8.2 ka BP event. The comparison between each
279 data set in Fig. 5 suggests that the decrease in rainfall in southwest China may indeed
280 be in response to Greenland cooling. Further analysis shows a weak-correlation
281 between Greenland ice core $\delta^{18}\text{O}$ and the reconstructed rainfall with a correlation
282 coefficient (R^2) of 0.47 (n=219) indicating a 1‰ drop in Greenland ice core $\delta^{18}\text{O}$
283 could lead to ~7% decrease in rainfall in southwest China. Though there is not enough

284 $\delta^{15}\text{N}$ data to reveal further correlations, it does indicate a drop of $3.3 \pm 1^\circ\text{C}$ when the
285 8.2 ka BP event occurred (Kobashi et al., 2007). As the reconstructed annual rainfall
286 record reveals a maximum decrease of 350 mm, the magnitude of rainfall response of
287 southwest China to Greenland cooling during 8.2 ka BP period could be assessed as
288 $110 \pm 30 \text{ mm}/^\circ\text{C}$.

289 5 Conclusions

- 290 1. Based on a comparison of two high-resolution stalagmite $\delta^{18}\text{O}$ records from
291 Dongge cave and Heshang cave along the monsoon moisture transport
292 pathway in China, a 10-yr moving average quantitative annual rainfall record
293 in southwest China is established during the 8.2 ka BP event.
- 294 2. Significant positive correlation between recent monitored drip water annual
295 average $\delta^{18}\text{O}$ differences from two caves along the monsoon moisture
296 transport pathway and the regional average annual rainfall from May 2011 to
297 April 2014 provides support for the reconstruction. Similar trends between the
298 reconstructed rainfall and stalagmite Mg/Ca ratios, another proxy of rainfall,
299 increase the confidence of the quantization of the rainfall record.
- 300 3. The reconstructed rainfall record shows that the annual rainfall in southwest
301 China decreased sharply by ~ 350 mm in ~ 70 years when the 8.2 ka BP event
302 occurred and experienced an extreme drying period lasting for ~ 50 years
303 during the central event. Compared with the modern instrumental records, the
304 averaged annual rainfall in southwest China during the 8.2 ka BP event is less
305 than that of present (1950 ~ 1990) by ~ 200 mm.
- 306 4. A comparison between reconstructed rainfall in southwest China and
307 Greenland ice core $\delta^{18}\text{O}$, an indicator of temperature, suggests that the rainfall
308 decrease in southwest China during the 8.2 ka BP period coupled with
309 Greenland cooling. A possible response rate of $110 \pm 30 \text{ mm}/^\circ\text{C}$ could be
310 presumed by the temperature drop derived from Greenland ice core $\delta^{15}\text{N}$ and
311 rainfall decrease from the reconstructed record.

312 **Acknowledgements.** This work was supported by NSFC Grants 41371216 and
313 41130207. We thank the editor, Prof. Dominik Fleitmann, and the two anonymous
314 reviewers for their valuable comments that greatly improved the manuscript. We also
315 thank Dr. Nick Belshaw for proofreading the manuscript.

316 References

317 Alley, R. B. and Ágústsson, A. M.: The 8k event: cause and consequences of a
318 major Holocene abrupt climate change, *Quaternary Sci. Rev.*, 24, 1123–1149, 2005.

319 Alley, R. B., Mayewski, P. A., Sowers, T., Stuiver, M., Taylor, K. C., and Clark, P. U.:
320 Holocene climatic instability: A prominent, widespread event 8200 yr ago, *Geology*,
321 25, 483–486, 1997.

322 Broccoli, A. J., Dahl, K. A., and Stouffer, R. J.: Response of the ITCZ to Northern
323 Hemisphere cooling, *Geophys. Res. Lett.*, 33, L01702, 2006.

324 Buizert, C., Gkinis, V., Severinghaus, J. P., He, F., Lecavalier, B. S., Kindler, P.,
325 Leuenberger, M., Carlson, A. E., Vinther, B., Masson-Delmotte, V., White, J. W. C.,
326 Liu, Z., Otto-Bliesner, B., and Brook, E. J.: Greenland temperature response to
327 climate forcing during the last deglaciation, *Science*, 345, 1177–1180, 2014.

328 Cheng, H., Fleitmann, D., Edwards, R. L., Wang, X., Cruz, F. W., Auler, A. S.,
329 Mangini, A., Wang, Y., Kong, X., Burns, S. J., and Matter, A.: Timing and structure
330 of the 8.2 kyr B.P. event inferred from $\delta^{18}\text{O}$ records of stalagmites from China,
331 Oman, and Brazil, *Geology*, 37, 1007–1010, 2009.

332 Chiang, J. C. H. and Bitz, C. M.: Influence of high latitude ice cover on the marine
333 Intertropical Convergence Zone, *Clim. Dynam.*, 25, 477–496, 2005.

334 Condron, A. and Winsor, P.: A subtropical fate awaited freshwater discharged from
335 glacial Lake Agassiz, *Geophys. Res. Lett.*, 38, L03705, 2011.

336 Daley, T. J., Thomas, E. R., Holmes, J. A., Street-Perrottd, F. A., Chapman, M. R.,
337 Tindall, J. C., Valdes, P. J., Loader, N. J., Marshall, J. D., Wolff, E. W.,
338 Hopley, P. J., Atkinson, T., Barberi, K. E., Fisherg, E. H., Robertson, I., Hughes,
339 P. D. M., and Roberts, C. N.: The 8200 yr BP cold event in stable isotope records
340 from the North Atlantic region, *Global Planet. Change*, 79, 288–302, 2011.

341 Dayem, K. E., Molnar, P., Battisti, D. S., and Roe, G. H.: Lessons learned from
342 oxygen isotopes in modern precipitation applied to interpretation of speleothem
343 records of paleoclimate from eastern Asia, *Earth Planet. Sc. Lett.*, 295, 219–230,
344 2010.

345 Ding, Y., Li, C., and Liu, Y.: Overview of the South China Sea Monsoon experiment.
346 *Adv. Atmos. Sci.*, 21, 343–360, 2004.

347 Dixit, Y., Hodell, D. A., Sinhab, R., and Petrie, C. A.: Abrupt weakening of the Indian
348 summer monsoon at 8.2 kyr B.P., *Earth Planet. Sc. Lett.*, 391, 16–23, 2014.

349 Domínguez-Villar, D., Fairchild, I. J., Baker, A., Wang, X., Edwards, R. L., and Cheng,
350 H.: Oxygen isotope precipitation anomaly in the North Atlantic region during the
351 8.2 ka event, *Geology*, 37, 1095–1098, 2009.

352 Duan, W., Ruan, J., Luo, W., Li, T., Tian, L., Zeng, G., Zhang, D., Bai, Y., Li, J., Tao,
353 T., Zhang, P., Baker, A., and Tan, M.: The transfer of seasonal isotopic variability
354 between precipitation and drip water at eight caves in the monsoon regions of
355 China, *Geochim. Cosmochim. Acta*, 183: 250–266, 2016.

356 Dykoski, C. A., Edwards, R. L., Cheng, H., Yuan, D., Cai, Y., Zhang, M., Lin, Y., Qing,
357 J., An, Z., and Revenaugh, J.: A high-resolution, absolute dated Holocene and
358 deglacial Asian monsoon record from Dongge Cave, China, *Earth Planet. Sc. Lett.*,
359 233, 71–86, 2005.

360 Ellwood, B. B. and Gose, W. A.: Heinrich H1 and 8200 yr B.P. climate events
361 recorded in Hall's Cave, Texas, *Geology*, 34, 753–756, 2006.

362 Fairchild, I. J. and Treble, P. C.: Trace elements in speleothems as recorders of
363 environmental change, *Quaternary Sci. Rev.*, 28, 449–468, 2009.

364 Ge, Q., Chu, F. Y., Xue, Z., Liu, J. P., Du, Y., and Fang, Y.: Paleoenvironmental
365 records from the northern South China Sea since the Last Glacial Maximum, *Acta*
366 *Oceanol. Sin.*, 29, 46–62, 2010.

367 Hede, M. U., Rasmussen, P., Noe-Nygaard, N., Clarke, A. L., Vinebrooke, R. D., and
368 Olsen, J.: Multiproxy evidence for terrestrial and aquatic ecosystem responses
369 during the 8.2 ka cold event as recorded at Højby Sø, Denmark, *Quaternary Res.*,
370 73, 485–496, 2010.

371 Hong, Y. T., Hong, B., Lin, Q. H., Shibatab, Y., Zhua, Y. X., Lengc, X. T., and Wang,
372 Y.: Synchronous climate anomalies in the western North Pacific and North Atlantic
373 regions during the last 14,000 years, *Quaternary Sci. Rev.*, 28, 840–849, 2009.

374 Hu, C., Henderson, G. M., Huang, J., Xie, S., Sun, Y., and Johnson K. R.:
375 Quantification of Holocene Asian monsoon rainfall from spatially separated cave
376 records, *Earth Planet. Sc. Lett.*, 266, 221–232, 2008a.

377 Hu, C., Henderson, G. M., Huang, J., Chen, Z., and Johnson, K. R.: Report of a three-
378 year monitoring programme at Heshang Cave, Central China, *Int. J. Speleol.*, 37 :
379 143–151, 2008b.

380 Khasnis, A. A. and Nettleman, M. D.: Global warming and infectious disease, *Arch.*
381 *Med. Res.*, 36, 689–696, 2005.

382 Kobashi, T., Severinghaus, J. P., Brook, E. J., Barnola, J. M., and Grachev, A. M.:
383 Precise timing and characterization of abrupt climate change 8200 years ago from
384 air trapped in polar ice, *Quaternary Sci. Rev.*, 26, 1212–1222, 2007.

385 LeGrande A. N. and Schmidt G. A.: Ensemble, water isotope-enabled, coupled
386 general circulation modeling insights into the 8.2 ka event, *Paleoceanography*, 23,
387 PA3207, 2008.

388 Liu, Y., Henderson, G. M., Hu, C., Mason, A. J. Charnley, N., Johnson, K. R., and Xie,
389 S.: Links between the East Asian monsoon and North Atlantic climate during the
390 8,200 year event, *Nat. Geosci.*, 6, 117–120, 2013.

391 Liu, Z., Wen, X., Brady, E.C., Otto-Bliesner, B., Yu, G. , Lu, H., Cheng, H., Wang, Y.,
392 Zheng, W., Ding, Y., Edwards, R.L., Cheng, J., Liu, W., and Yang, H.: Chinese cave
393 records and the East Asia Summer Monsoon, *Quaternary Sci. Rev.*, 83, 115-128,
394 2014.

395 Ljung, K., Björck, S., Renssen, H., and Hammarlund, D.: South Atlantic island record
396 reveals a South Atlantic response to the 8.2 kyr event, *Clim. Past*, 4, 35–45, 2008.

397 Martrat, B., Grimalt, J. O., Lopez-Martine, C., Cacho, I., Sierro, F. J., Flores, J. A.,
398 Zahn, R., Canals, M., Curtis, J. H., and Hodell, D. A.: Abrupt temperature changes
399 in the western Mediterranean over the past 250,000 years, *Science*, 306, 1762–1765,
400 2004.

401 Mischke, S. and Zhang, C. J.: Holocene cold events on the Tibetan Plateau, *Global*

402 Planet. Change, 72, 155–163, 2010.

403 Morrill C., Anderson, D. M., Bauer, B. A., Buckner, R., Gille, E. P., Gross, W. S.,
404 Hartman, M., and Shah, A.: Proxy benchmarks for intercomparison of 8.2 ka
405 simulations, *Clim. Past*, 9, 423–432, 2013.

406 Morrill, C., Wagner, A. J., Otto-Bliesner, B. L., and Rosenbloom, N.: Evidence for
407 significant climate impacts in monsoonal Asia at 8.2 ka from multiple proxies and
408 model simulations, *J. Earth Environ.*, 2, 426–441, 2011.

409 Pall, P., Allen, M. R., and Stone, D. A.: Testing the Clausius–Clapeyron constraint on
410 changes in extreme precipitation under CO₂ warming, *Clim. Dynam*, 28, 351–363,
411 2007.

412 Prasad, S., Witt, A., Kienel, U., Dulski, P., Bauer, E., and Yancheva, G.: The 8.2 ka
413 event: Evidence for seasonal differences and the rate of climate change in western
414 Europe, *Global Planet. Change*, 67, 218–226, 2009.

415 Rahmstorf, S.: A semi-empirical approach to projecting future sea-level rise, *Science*,
416 315, 368–370, 2007.

417 Snowball, I., Muscheler, R., Zillén, L., Sandgren, P., Stanton, T., and Ljung, K.:
418 Radiocarbon wiggle matching of Swedish lake varves reveals asynchronous climate
419 changes around the 8.2 kyr cold even, *Boreas*, 39, 720–733, 2010.

420 Stuiver, M., Grootes, P. M., and Brazunias, T. F.: The GISP2 $\delta^{18}\text{O}$ record of the past
421 16,500 years and the role of the Sun, ocean and volcanoes, *Quaternary Res.*, 44,
422 341–354, 1995.

423 Szeroczyńska, K. and Zawisza, E.: Records of the 8200 cal BP cold event reflected in
424 the composition of subfossil Cladocera in the sediments of three lakes in Poland,
425 *Quatern. Int.*, 233, 185–193, 2011.

426 Thomas, E. R., Wolff, E. W., Mulvaney, R., Steffensen, J. P., Johnsen, S. J.,
427 Arrowsmith, C., White, J. W.C., Vaughn, B., and Popp, T.: The 8.2 ka event from
428 Greenland ice cores, *Quaternary Sci. Rev.*, 26, 70–81, 2007.

429 Tremaine, D. M. and Froelich, P.N.: Speleothem trace element signatures: A
430 hydrologic geochemical study of modern cave dripwaters and farmed calcite,
431 *Geochim. Cosmochim. Acta*, 121, 522–545, 2013.

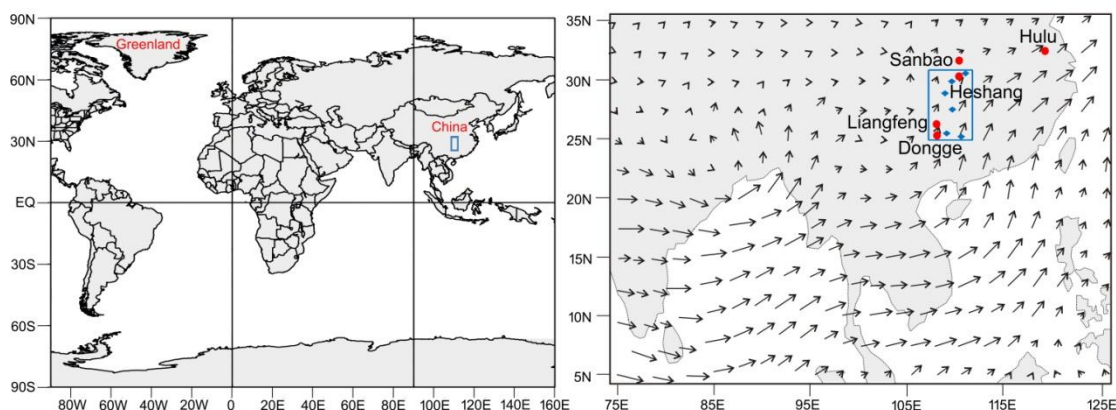
432 Walther, G. R., Post, E., Convey, P., Menzel, A., Parmesan, C., Beebee, T. J. C.,
433 Fromentin, J. M., Hoegh-Guldberg, O., and Bairlein, F.: Ecological responses to
434 recent climate change, *Nature*, 416, 389–395, 2002.

435 Wang, Y., Cheng, H., Edwards, R. L., He, Y., Kong, X., An, Z., Wu, J., Kelly, M. J.,
436 Dykoski, C. A., and Li, X.: The Holocene Asian Monsoon: links to solar changes
437 and North Atlantic climate, *Science*, 308, 854–857, 2005.

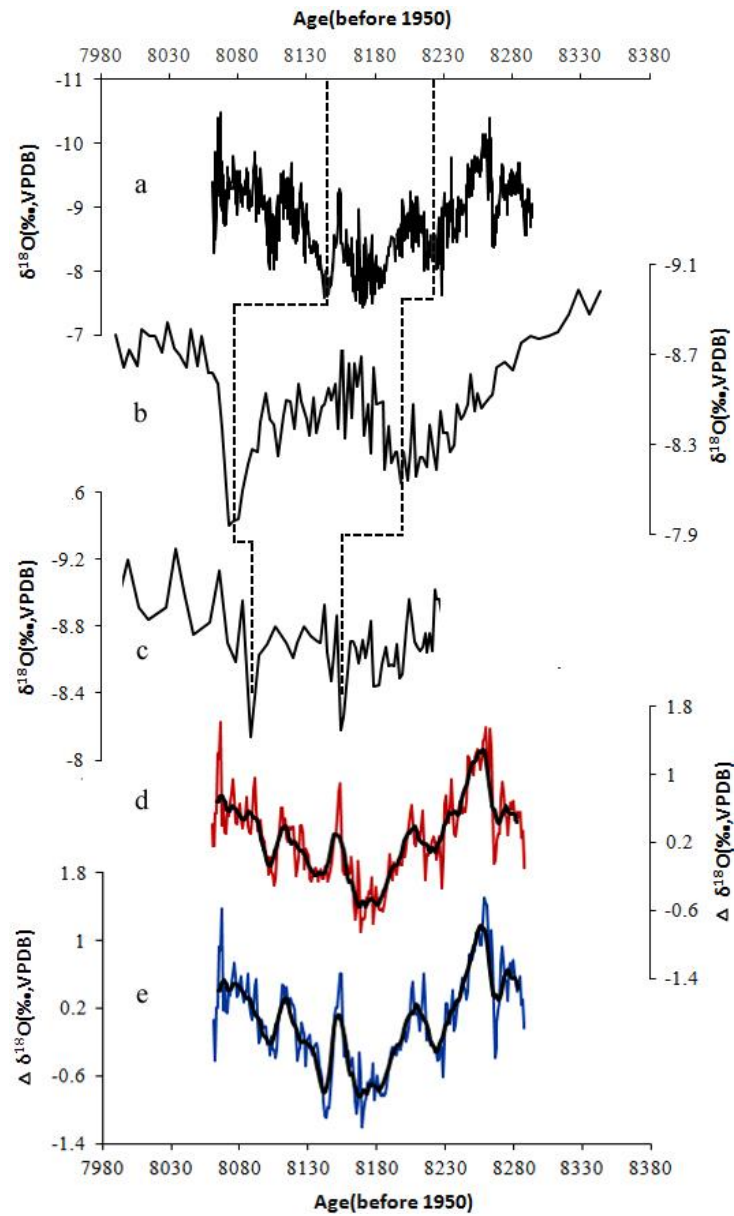
438 Wu, J., Wang, Y., Cheng, H., Kong, X., and Liu, D.: Stable isotope and trace element
439 investigation of two contemporaneous annually-laminated stalagmites from
440 northeastern China surrounding the “8.2 ka event”, *Clim. Past*, 8, 1497–1507, 2012.

441 Yu, X., Zhou, W., Franzen, L. G., Feng, X., Peng, C., and Jull, A. J. T.: High-
442 resolution peat records for Holocene monsoon history in the eastern Tibetan Plateau,
443 *Sci. China Earth Sci.*, 49, 615–621, 2006.

444 Zeng, G., Luo, W., Wang, S., and Du, X.: Hydrogeochemical and climatic
 445 interpretations of isotopic signals from precipitation to drip waters in Liangfeng
 446 Cave, Guizhou Province, China, *Environ. Earth Sci.*,74, 1509-1519, 2015.
 447 Zheng, Y., Zhou, W., Xie, S., and Yu, X.: A comparative study of n-alkane biomarker
 448 and pollen records: an example from southern China, *Chinese Sci. Bull.*, 54, 1065–
 449 1072, 2009.
 450 Zheng, Y., Kissel, C., Zheng, H., Lajb, C., and Waang, K.: Sedimentation on the inner
 451 shelf of the East China Sea: Magnetic properties, diagenesis and paleoclimate
 452 implications, *Mar. Geol.*, 268, 34–42, 2010.



453
 454 Figure 1. Location maps. The left map shows the location of Greenland and southwest China (blue
 455 box). The right map shows the location of Heshang cave and other Chinese caves (red points), with
 456 main feature of the summer monsoon marked. Smaller arrows reflect moisture transport and
 457 direction averaged over the whole atmosphere (Ding et al., 2004). The blue box indicates the
 458 specific region for which comparison of Heshang and Dongge allows rainfall reconstruction, and
 459 the blue diamond patterns show the location of six modern rainfall stations detailed in Hu et
 460 al.(2008) .



461

462

463 Figure 2. Original $\delta^{18}\text{O}$ stalagmite records adopted in this paper displayed with $\Delta\delta^{18}\text{O}$

464

sequences between stalagmites from Dongge and Heshang. a. HS4 $\delta^{18}\text{O}$ record from Heshang

465

cave(Liu et al., 2013); b. DA $\delta^{18}\text{O}$ record from Dongge cave(Cheng et al., 2009); c. D4 $\delta^{18}\text{O}$

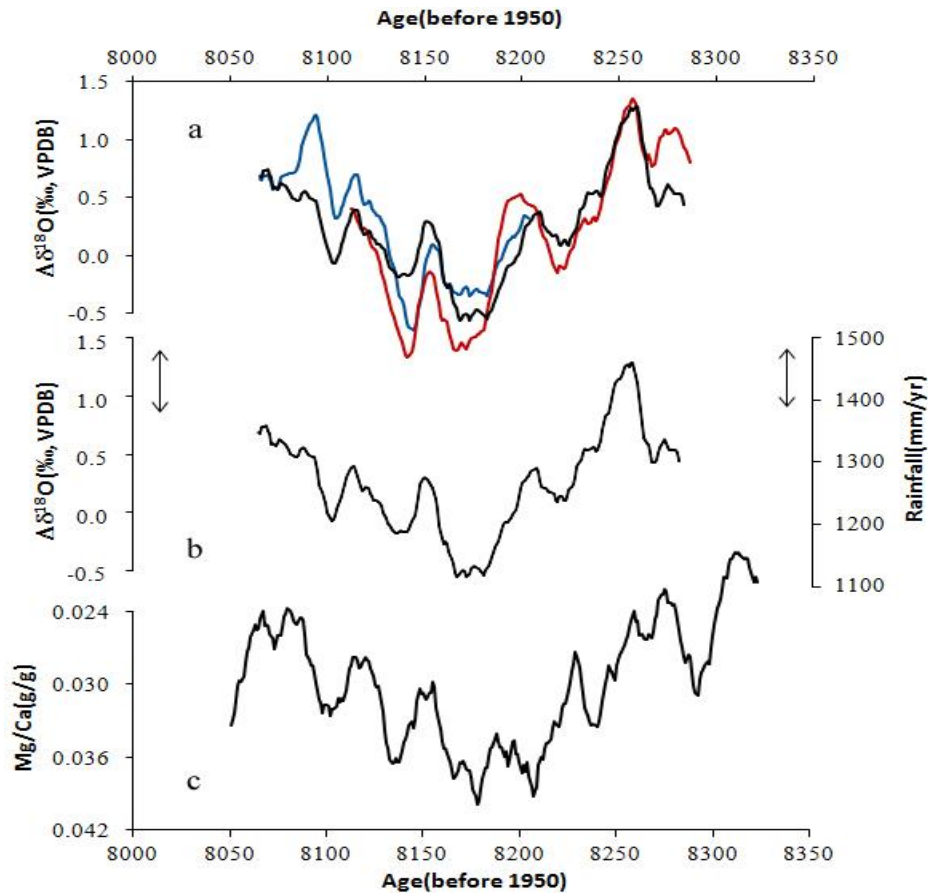
466

record from Dongge cave (Cheng et al., 2009); d. $\Delta\delta^{18}\text{O}$ between DA and HS4 (red) with a 10-

467

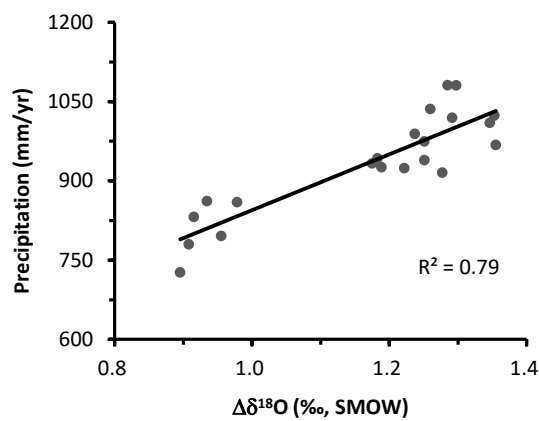
year moving average(black); e. $\Delta\delta^{18}\text{O}$ between D4 and HS4 (blue) with a 10-year moving

average (black). The dashed lines show matched peaks from each original record.



468

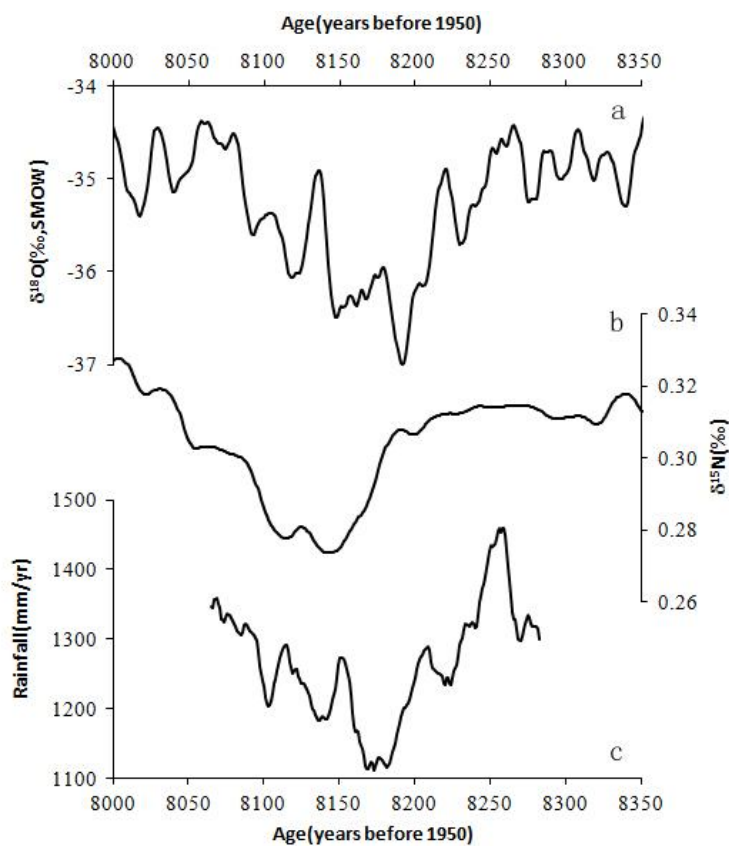
469 Figure 3. 10-yr moving average records during the 8.2 ka BP period. a. $\Delta \delta^{18}\text{O}$ records between
 470 HS4 and DA with unchanged chronology (black), shifting DA 50-yr younger (blue) and 50-yr
 471 older (red); b. $\Delta \delta^{18}\text{O}$ record between HS4 and DA and reconstructed annual rainfall in
 472 southwest China with error bars indicated; c. Mg/Ca ratios of HS4 shown on inverted scales,
 473 which reveals a similar trend to the rainfall sequence, increasing the confidence of the
 474 quantization of the reconstructed record.



475

476 Figure 4. Correlation analysis between mean annual precipitation and drip water $\delta^{18}\text{O}$
 477 difference from 2-month delayed LF6 and 4-month delayed HS4 from May 2011 to April
 478 2014. The $\Delta \delta^{18}\text{O}$ data are calculated from monthly monitored data from Liangfeng cave and
 479 Heshang cave (Duan et al., 2016). The annual precipitation data are the average from six sites
 480 between Dongge cave and Heshang cave detailed in Hu et al. (2008a) and the original

481 monthly rainfall data are from <http://www.wunderground.com/history/>. The correlation factor
482 of 0.79 indicates a significant positive correlation between regional annual rainfall and annual
483 $\Delta\delta^{18}\text{O}$.
484



485
486 Figure 5. Records from Greenland ice core $\delta^{18}\text{O}$ (Thomas et al., 2007) (a), Greenland ice core
487 $\delta^{15}\text{N}$ (Kobashi et al., 2007) (b) and the reconstructed annual rainfall from this study(c) during
488 the 8.2 ka BP event. Three sequences show a similar pattern indicating the decrease in rainfall
489 in southwest China was coupled with Greenland cooling during the 8.2 ka BP event.
490